JACS
JOURNAL OF THE AMERICAN CHEMICAL SOCIETY
pubs.acs.org/JACS
Article

Three-Motif Molecular Junction Type Covalent Organic Frameworks for Efficient Photocatalytic Aerobic Oxidation

Ming-Yi Yang, Shuai-Bing Zhang, Mi Zhang, Ze-Hui Li, Yu-Fei Liu, Xing Liao, Meng Lu,* Shun-Li Li, and Ya-Qian Lan*

Cite This: J. Am. Chem. Soc. 2024, 146, 3396−3404

Read Online

ACCESS | Metrics & More | Article Recommendations | Supporting Information

ABSTRACT: Covalent organic frameworks (COFs), with the features of flexible structure regulation and easy introduction of functional groups, have aroused broad interest in the field of photocatalysis. However, due to the low light absorption intensity, low photoelectron conversion efficiency, and lack of suitable active sites, it remains a great challenge to achieve efficient photocatalytic aerobic oxidation reactions. Herein, based on reticular chemistry, we rationally designed a series of three-motif molecular junction type COFs, which formed dual photosensitizer coupled redox molecular junctions containing multifunctional COF photocatalysts. Significantly, due to the strong light adsorption ability of dual photosensitizer units and integrated oxidation and reduction features, the PY-BT COF exhibited the highest activity for photocatalytic aerobic oxidation. Especially, it achieved a photocatalytic benzylamine conversion efficiency of 99.9% in 2.5 h, which is much higher than that of the two-motif molecular junctions with only one photosensitizer or redox unit lacking COFs. The mechanism of selective aerobic oxidation was studied through comprehensive experiments and density functional theory calculations. The results showed that the photoinduced electron transfer occurred from PY and then through triphenylamine to BT. Furthermore, the thermodynamics energy for benzylamine oxidation on PY-BT COF was much lower than that for others, which confirmed the synergistic effect of dual photosensitizer coupled redox molecular junction COFs. This work provided a new strategy for the design of functional COFs with three-motif molecular junctions and also represented a new insight into the multifunctional COFs for organic catalytic reactions.

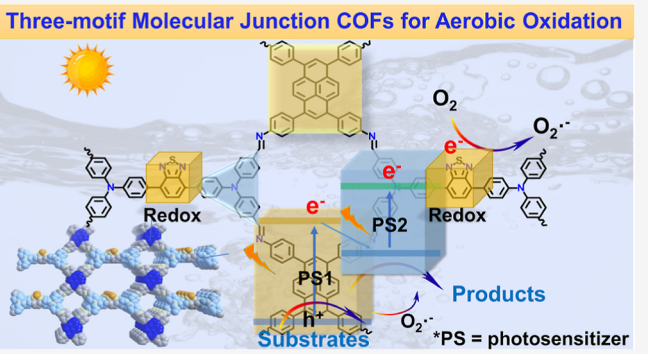

INTRODUCTION

The energy and environmental crisis has been a critical issue of concern all over the world.[1,2] Rational use of green and clean energy, such as solar energy, plays an important role in solving energy and environmental problems. From a green and sustainable perspective, solar-driven photocatalysis has become an ideal alternative to traditional thermal synthesis methods.[3,4] As one of the broad categories of the photocatalytic organic transform reaction, aerobic oxidation was involved in a wide range of photochemical transformations that allow the facile preparation of various useful commodity chemicals and functional building blocks.[5−10] In the field of aerobic oxidation, benzylamines oxidation to their derivatives plays a crucial part in the chemical and polymer industries and also provides an important resource in the synthesis of a crowd of nitrogen-containing functional molecules.[11−15] As previously reported, there were two main types of photocatalyst materials for aerobic oxidation (Scheme 1): (1) inorganic or organic semiconductor catalysts such as metal oxides, metal sulfides, and carbon nitride materials and organic molecular catalysts including Ru(II) and Ir(III) complexes[16−18] and (2) heterojunction catalysts: such as inorganic−inorganic hybrids, inorganic−organic hybrids, and multicomponent composite materials including metal organic frameworks or cluster-based frameworks.[19] All of the above catalysts have been largely explored in photocatalytic aerobic oxidation reactions. However, many reported photocatalysts have various limitations, thus causing low conversion efficiency. Especially, the photocatalytic benzylamine oxidation still needs in-depth exploration to find photocatalysts with a well-defined structure, a strong response to visible light, strong redox ability, good recycling, and strong substrate conversion ability.[20−25] Unfortunately, it is always difficult with single semiconductor or two-unit heterojunction type materials to achieve precise structural adjustment on the oxidative and reductive

Received: November 15, 2023
Revised: January 6, 2024
Accepted: January 8, 2024
Published: January 24, 2024

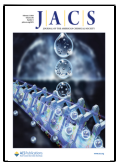

https://doi.org/10.1021/jacs.3c12724
J. Am. Chem. Soc. 2024, 146, 3396−3404

Scheme 1. Schematic and the Concept of Designing Three-Motif Molecular Junction Type Catalysts for Photocatalytic Aerobic Oxidations

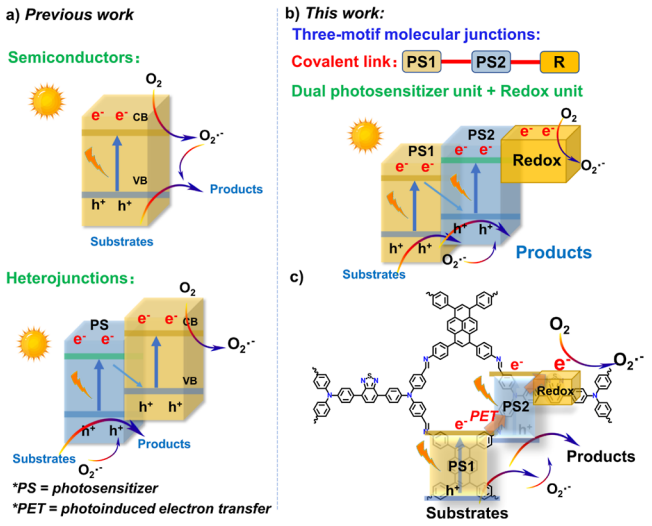

components from the molecular level, with them also suffering from a narrow light absorption range, a low photoelectron conversion efficiency, and a lack of suitable active sites. Therefore, designing a new regulable catalyst model to achieve multidimensional structure control will be the direction of the future development of photocatalysts.[26,27]

The molecular junction catalyst, which refers to the molecular structure formed by two functional groups such as oxidative and reductive agents, is one of the ideal types of catalyst to fulfill the coupling reaction. The two-motif molecular junction catalysts were first developed in our recent studies, which innovatively realized the coupling of oxidative and reductive reactions in one system, and were successfully used for artificial photosynthesis, photocatalytic hydrogen peroxide synthesis, organic photocatalysis, and so on.[28−32] However, further implementation of three or more functional groups to break through the limitations of multifunctionality for two-motif molecular junction catalysts has not been studied. The functional groups such as photosensitizer units, electron transport units, redox catalytic centers, and so on can be simultaneously introduced to the molecular junction materials to couple efficient light absorption, photoelectron conversion, and highly active catalytic sites.[33−40] Therefore, the modulation of multifunctional catalysts can be realized on the basis of multiple-motif molecular junction materials. The key issue that needs to be solved urgently is selecting a suitable platform to realize the above design concept.

Covalent organic frameworks (COFs), a new type of emerging crystalline organic porous materials assembled by covalent bonds with customizable atomic-level structures and a porous environment, have attracted much attention since their first report in 2005.[41−43] Adequate studies of COFs based on rational molecular design were reported, especially in the field of photocatalysis, aimed to improve their visible light absorption ability, carrier mobility, and activity of the reaction center, which facilitate the developments of high-performance COFs. However, although it is an ideal platform for achieving a multifunctional design, rarely have COFs achieved the above features simultaneously. Among many photocatalytic motifs, the pyrene and triphenylamine photosensitizers played an excellent donor group with outstanding optical proprieties such as a high quantum yield, a long average lifetime, and ease of the forming excimer. Due to its remarkable optical properties, pyrene has been used to prepare a wide range of photocatalyst materials.[44] Besides, the benzothiadiazole-based organic building block with five-membered heterocyclic compounds containing two nitrogen atoms and one sulfur atom, as well as two double bonds, forming an aromatic ring, which could provide a reduction site in redox reactions.[45,46]

In this work, we put out a strategy to rationally design a series of three-motif molecular junction catalysts, which formed a kind of double photosensitizer and an oxidation−reduction molecular junction containing COFs. Significantly, these three-motif molecular junction COFs were successfully used for photocatalytic aerobic oxidations. In these COFs, the pyrene and triphenylamine units were recognized as effective

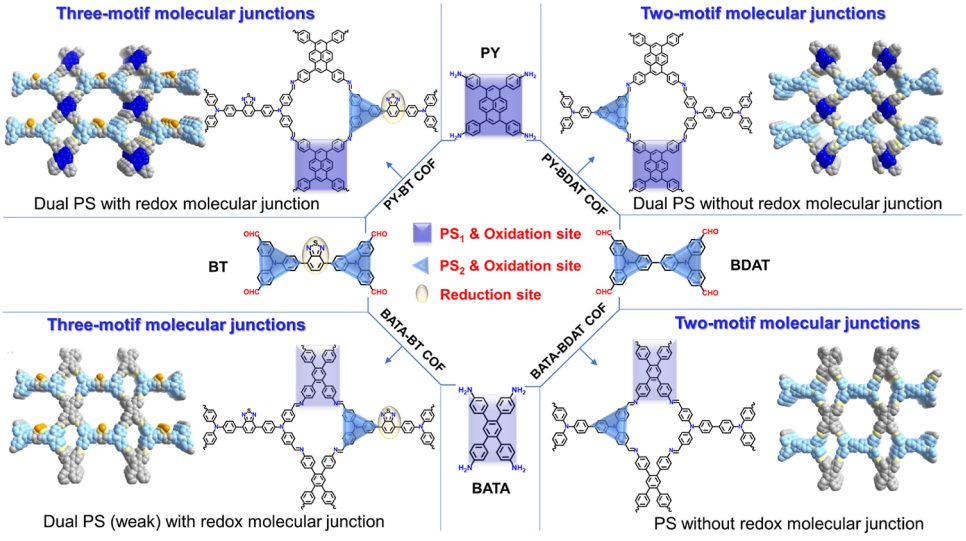

Figure 1. Schematic of the synthesis and structure of dual photosensitizer coupled redox molecular junction COFs, including the PY-BT COF, PY-BDAT COF, BATA-BT COF, and BATA-BDAT COF. *PS = photosensitizer; the purple block represents PS_1 and the oxidation site; the blue block represents PS_2 and the oxidation site; and the yellow block represents the redox site.

https://doi.org/10.1021/jacs.3c12724
J. Am. Chem. Soc. 2024, 146, 3396−3404

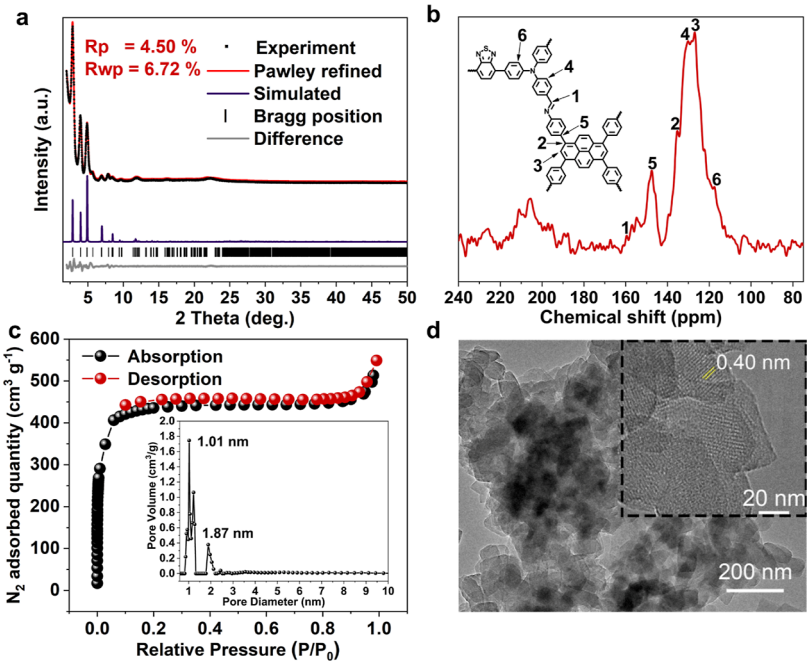

Figure 2. Structure and characterization of the PY-BT COF. (a) Experimental and simulated PXRD patterns. (b) ^{13}C ssNMR of the PY-BT COF. (c) N_2 adsorption analysis. (d) TEM images of the PY-BT COF.

photosensitizers and photooxidation sites, and thiadiazole groups were used as reduction sites. At the same time, COFs with two-motif molecular junctions, which contained only one photosensitizer site, a double photosensitizer site without a reducing site, and only one double photosensitizer site, were constructed and synthesized as comparison samples. As a proof of concept, the double photosensitizer coupled redox heterojunction-based three-motif molecule-based COFs were studied for the photocatalytic oxidative reaction of benzylamine to imines. The results showed that benzylamine could be completely converted into coupling imine products with a conversion efficiency of 99.9% in 2.5 h and high selectivity, and the conversion rate was the highest compared with that of the other three samples, indicating that the double photosensitizer redox three-motif molecule junction COFs have better photocatalytic oxidation reaction activity.

RESULTS AND DISCUSSION

Synthesis and Structure of COFs. As shown in Figure 1 and the Experimental Section in the Supporting Information, a [4 + 4] condensation reaction was applied to synthesize the above-designed COFs. Specifically, the PY-BT COF was synthesized by a Schiff base condensation reaction between 4,4′,4″,4‴-((benzo[c][1,2,5]thiadiazole-4,7-diylbis(4,1-phenylene))bis(azanetriyl))tetrabenzaldehyde (BT) and 4,4′,4″,4‴-(1,3,6,8-pyrenetetrayl)tetrakis[benzenamine] (PY). The PY-BT COF was obtained as a dark orange powder with a yield of 86.3%, while the BATA-BT COF was obtained as a light orange solid with a yield of 79.3%. As a control, 4,4′,4″,4‴-([1,1′-biphenyl]-4,4′-diyldinitrilo)tetrakis (BDAT) is selected as a knot with PY and BATA, composing the other two new COFs, which are called PY-BDAT COF and BATA-BDAT COF.

The crystalline structures of the PY-BT COF and BATA-BT COF and the contrast samples PY-BDAT COF and BATA-BDAT COF were first studied by the powder X-ray diffraction (PXRD) experiment and analysis by theoretical structural simulations, as shown in Figures 2a and S5−S7. For the PY-BT COF, the experimental PXRD patterns matched well with the calculated results from the AA stacking mode, while a comparison of the AB stacking mode showed significant deviations (Figure S1), and for the BATA-BT COF, PY-BDAT COF, and BATA-BDAT COF, please see the Supporting Information, Figure S2−S4. The PY-BT COF exhibits intense peaks at 2.89, 4.04, 4.65, 6.60, and 8.68°, which can be assigned to the 100, 010, 110, 210, and 300 faces, respectively. The unit cell parameters were obtained after a geometrical energy minimization and refinement based PY-BT COF 2D net with AA stacking mode with lattice parameters of a = 32.3579 Å, b = 23.9344 Å, c = 3.8665 Å, α = 113.0045°, β = 72.2050°, γ = 90.2160°. The porosity of activated BT-COFs and BDAT-COFs was measured through N_2 adsorption−desorption at 77 K (Figure 2c). The sorption curves of the PY-BT COF and BATA-BT COF both were type I isotherms. The BET surface areas of the PY-BT COF and BATA-BT COF are 1705.73 and 1347.04 m^2/g, respectively. Pore size distribution was also investigated to obtain the micro porosity properties of the PY-BT COF with aperture sizes of 1.87 and 1.01 nm, and the BATA-BT COF has the aperture pore sizes of 1.80 and 1.21 nm (Figures S12 and S15). The PXRD patterns and the BET surface areas of the PY-BDAT COF and BATA-BDAT COF could be found in the Supporting Information (Figures S13, S14, S16, and S17).

The chemical structure of the COFs was characterized by Fourier transform infrared (FT-IR) spectroscopy and solid-state nuclear magnetic resonance (ssNMR). The FT-IR spectra of the COFs showed the appearance of C═N stretching vibration bands at 1621 cm^{-1} and the disappearance of C═O stretching signals at 1698 cm^{-1}, respectively, indicating the consumption of the starting materials and successful polymerization (Figures S8−S11). The solid-state ^{13}C NMR spectrum of the PY-BT COF showed a low field signal at ∼154.9 ppm, which was attributed to the carbon atom of the C═N bond (Figure 2b). All of these results confirmed the successful

https://doi.org/10.1021/jacs.3c12724
J. Am. Chem. Soc. 2024, 146, 3396−3404

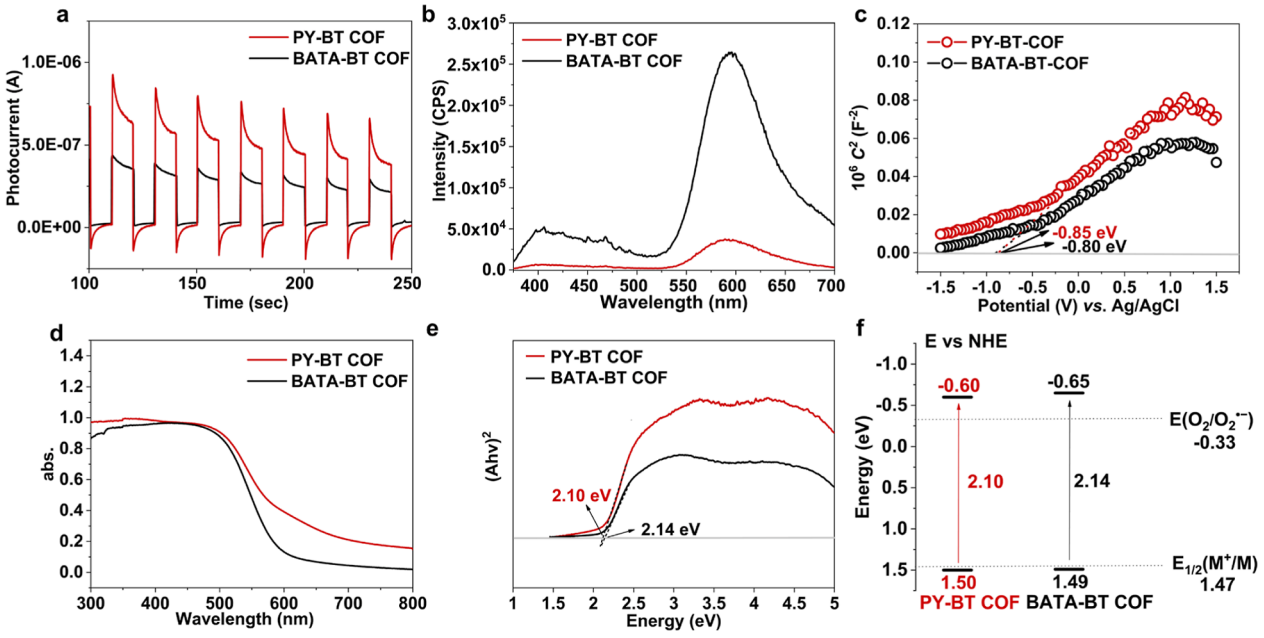

Figure 3. Optical characterization of PY-BT COF and BATA-BT COF. (a) Transient photocurrent responses of the PY-BT COF and BATA-BT COF. (b) PL spectra of PY-BT COF and BATA-BT COF in the solid state. (c) Mott−Schottky plots of the PY-BT COF and BATA-BT COF. (d) UV/visible absorption spectra of the PY-BT COF and BATA-BT COF. (e) Tauc plots of PY-BT COF and BATA-BT COF. (f) Schematic energy band structures of PY-BT COF and BATA-BT COF.

covalent condensations required for these COFs (Figures S18−S20).

In order to study the thermal stability of COFs, thermogravimetric analysis (TGA) of these COFs was performed under a nitrogen atmosphere and showed no obvious change up to ∼290 °C for the PY-BT COF (Figure S28), and BATA-BT COF (Figure S29). TGA of these four COFs performed under an air atmosphere can be found in the Supporting Information (Figures S30−S35), which showed that new framework materials PY-BT COF and BATA-BT COF have excellent thermal stability. Furthermore, the chemical stability was tested by immersing them in solvents such as *N*,*N*-dimethylformamide, dichloromethane, petroleum ether, water, aqueous HCl (pH = 1), and NaOH (pH = 14) solutions at room temperature for 3 days. The PXRD pattern still displayed strong diffraction signals (Figures S36 and S37).

The crystalline morphology of these COFs was further analyzed through scanning electron microscopy (SEM) and transmission electron microscopy (TEM). The TEM images and SEM images of the PY-BT COF and BATA-BT COF showed that two benzothiadiazole-based COFs exist in a similar block crystal (Figures 2d, S21, S24, and S25) The contrast sample PY-BDAT COF and BATA-BDAT COF have different SEM images that exist in the sheet structure (Figures S26 and S27), and the TEM images of the PY-BDAT COF and BATA-BDAT COF can be found in the Supporting Information (Figures S22 and S23). As shown in Figure 2d, the structural characteristics of the PY-BT COF were then analyzed by high-resolution TEM (HRTEM). The PY-BT COF displayed clear lattice fringes of the (001) crystal face, which also confirmed the simulated crystal structure.

Optical and Physical Characterization of COFs. To study the behaviors of light harvesting of these COFs, the transient photocurrent response of these COFs was first obtained.[47,48] Figure 3a shows the transient photocurrent response of the PY-BT COF and BATA-BT COF, where compared to that of the BATA-BT COF, the PY-BT COF shows a much higher photocurrent response, and this evidence suggests that it has a more efficient photoelectron conversion capability. As shown in Figure 3b, the photoluminescence intensity of the PY-BT COF was poorer than that of the BATA-BT COF, implying that the recombination of the photogenerated carrier of the PY-BT COF was weaker than that of the BATA-BT COFs, which is beneficial for the catalytic reduction reaction. Solid-state UV/vis absorption spectra were obtained to study the light absorption capacity of these COFs. The results of the PY-BT COF and BATA-BT COF exhibit a broad visible adsorption range up to visible light (400−800 nm) (Figure 3d), and it shows that the PY-BT COF and BATA-BT COF are suitable photocatalytic materials. The PY-BDAT COF and BATA-BDAT COF show strong visible light absorption capacity (Figure S43). To suggest the electronic structure characteristics of these COFs, it is observed from Tauc plots (Figure 3e) that the corresponding band gaps (E_g) were determined to be 2.10 eV for the PY-BT COF and 2.14 eV for the BATA-BT COF. The electrochemical Mott−Schottky measurements (Figure 3c) were performed to obtain the relative positions of the conduction band (CB) and valence band (VB), and the results reveal that the average flat band positions of the PY-BT COF and BATA-BT COF are −0.80 and −0.85 V (vs Ag/AgCl, −0.60 and −0.65 V vs NHE), respectively.[49]

Since the bottom of the CB in n-type semiconductors is commonly close to the flat-band potential, the CB locations of the PY-BT COF and BATA-BT COF were estimated to be −0.60 and −0.65 eV, respectively. The VB position at 1.50 eV for the PY-BT COF and 1.49 eV for the BATA-BT COF could be obtained from the corresponding band gap energy (Figure 3f).[50−53] More information is displayed in the Supporting Information, including the PL of the PY-BDAT COF and BATA-BDAT COF (Figure S40), a series of optical characterizations, and the calculation of the schematic energy band

https://doi.org/10.1021/jacs.3c12724
J. Am. Chem. Soc. 2024, 146, 3396−3404

structure of the PY-BDAT COF and BATA-BDAT COF (Figures S38, S39, S41, S42, S44, and S45).

Photocatalytic Performance toward Oxidative Coupling of Benzylamines. The photocatalytic activity of the PY-BT COF and the other three COFs was then explored for aerobic oxidation of benzylamine. First of all, we chose CH_3CN as the solvent and benzylamine as the model substrate. Benzylamine and a series of benzylamine derivatives were selected as substrates to measure the photocatalytic ability of the PY-BT COF and the other three COF photocatalysts. Interestingly, the results showed that benzylamine and its derivatives could all be transformed to coupling products of benzylamine and its derivatives for these COF catalysts. Most importantly, the PY-BT COF performed much better than the contrast sample BATA-BT COF, PY-BDAT COF, and BATA-BDAT COF in conversion of the substrate at the same time. From the photocatalytic performance toward oxidative coupling of benzylamines (Figure 4a), it took the PY-BT COF 2.5 h to transform benzylamine to *N*-benzylbenzaldimine entirely. In the same duration of 2.5 h, the BATA-BT COF could achieve a conversion of 69.7%, the PY-BDAT COF achieved a conversion of 47.1%, and the BATA-BDAT COF achieved a conversion of 54.3%. As represented, the PY-BT COF consistently demonstrates premium catalytic activities in the oxidation of a series of benzylamine derivatives (Figures S47–S54) regardless of their electron-donating groups (−Me and −OMe) or electron-withdrawing groups (−F and −Cl). Impressively, the PY-BT COF also shows strong photocatalytic activities in transforming a secondary amine, for example, 1,2,3,4-tetrahydroisoquinoline, into the corresponding imine in 99.9% yield. Furthermore, the isolated yields of products for the PY-BT COF as a photocatalyst were calculated, and the results showed that >98% yields can be achieved for all benzylamine substrates. The gram−scale reaction test for the PY-BT COF catalyst showed that 1.24 g of pure *N*-benzylidenebenzylamine products can be isolated when using 1.5 g of benzylamine as a substrate (Figures S55–S62).

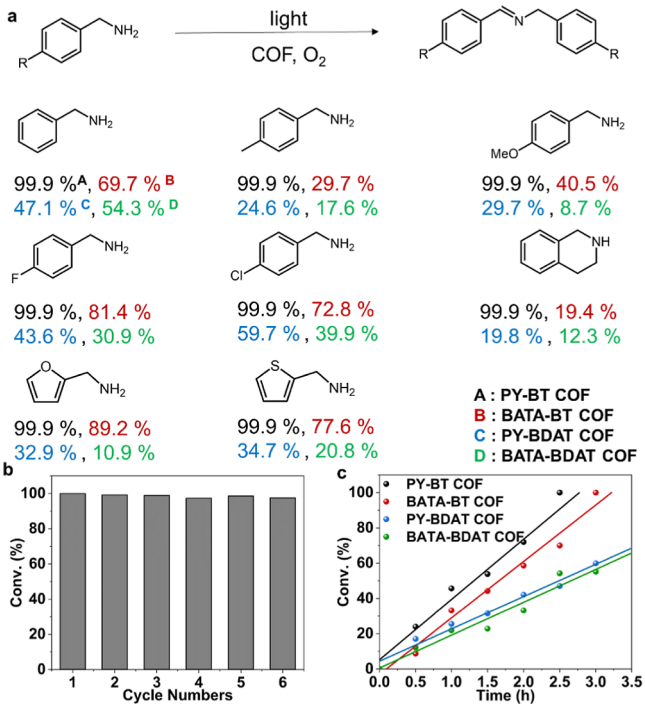

Figure 4. Photocatalytic performance toward the oxidative coupling of benzylamines. (a) Photocatalytic benzylamine oxidative coupling reactions and the percent conversions of COFs at the time of complete conversion by the PY-BT COF. The black font A is for the PY-BT COF; the red font B is for the BATA-BT COF; the blue font C is for the PY-BDAT COF; and the green font D is for the BATA-BDAT COF. (b) Reusability of the PY-BT COF. (c) Benzylamine conversion occurred at different times for COFs.

As shown in the recycling experiments, the PY-BT COF shows good catalytic performance and excellent stability for six cycle patterns, providing evidence that the crystallinity was still consistent with the initial state after the photocatalytic reaction (Figures 4b, S63, and S64). To explore the relationship of the conversation and time of these COFs, we chose benzylamine as a substrate, and then, reaction solutions were extracted and analyzed every half an hour (Figure 4c). The result showed that the PY-BT COF as a photocatalyst has the best activity. It is considered the double photosensitizer redox molecule COFs had better photocatalytic oxidation reaction activity.[54]

Studies on the Photocatalytic Reaction Mechanism. In order to study the photocatalytic reaction mechanism and investigate structure−function relationships, the experiments including electron paramagnetic resonance (EPR) test and theoretical research including density functional theory (DFT) calculations were performed.[55−57] EPR studies can evaluate the ability of materials to produce reactive oxygen species and free radicals. Compared with the BATA-BT COF, the PY-BT COF showed a more significant enhancement of the EPR signal after light irradiation, which proves that the PY-BT COF is more efficient in producing charge carriers than the BATA-BT COF under light irradiation. Once again, it was proved that the PY-BT COF has the advantage in photocatalytic aerobic oxidation reactions (Figures 5a,b). In addition, the photocatalytic oxidative coupling reaction mechanism of the PY-BT COF and BATA-BT COF was investigated by EPR measurements and a set of trapping experiments. We used 5,5-dimethylpyrroline-*N*-oxide (DMPO) and 2,2,6,6-tetramethyl-4-piperidone (4-oxo-TEMP) to capture and quantify $O_2^{\bullet-}$ and $^1O_2$, respectively. In our system, the PY-BT COF has a stronger ability to activate O_2 to $O_2^{\bullet-}$ or $^1O_2$ than other COFs. It is observed from the figure that the PY-BT COF has more obvious $O_2^{\bullet-}$ and $^1O_2$ signals than the BATA-BT COF.[58−61] These results showed that the dual photosensitizer coupled redox molecular junction COFs showed superior ability to others with one photosensitizer or no redox sites in catalyzing aerobic oxidation reactions.

Based on the above results, we proposed a dual photosensitizer excited oxidative coupling mechanism of benzylamine under visible light irradiation for these COFs, as shown in Figure 5c: under visible light irradiation, two photosensitizer units, that is, pyrene and triphenylamine, were simultaneously excited, and the photogenerated electrons were transferred to the benzothiadiazole unit, at which time O_2 would react with photogenerated electrons to form $O_2^{\bullet-}$ and $^1O_2$ was generated via energy transfer from COFs. At the same time, the adsorbed benzylamine molecules are oxidized by photogenic holes to form benzylamine radical cations. $O_2^{\bullet-}$ extracts protons from the benzylamine radical cation and yields Ph−CH═NH and H_2O_2. Then, H_2O_2 reacts with the new benzylamine molecule and generates Ph−CH═NH, which further reacts with the new benzylamine molecule to produce benzalaniline as a final product along with ammonia liberation. On the other hand, $^1O_2$ subsequently captures two protons from benzylamine, as a

https://doi.org/10.1021/jacs.3c12724
J. Am. Chem. Soc. 2024, 146, 3396−3404

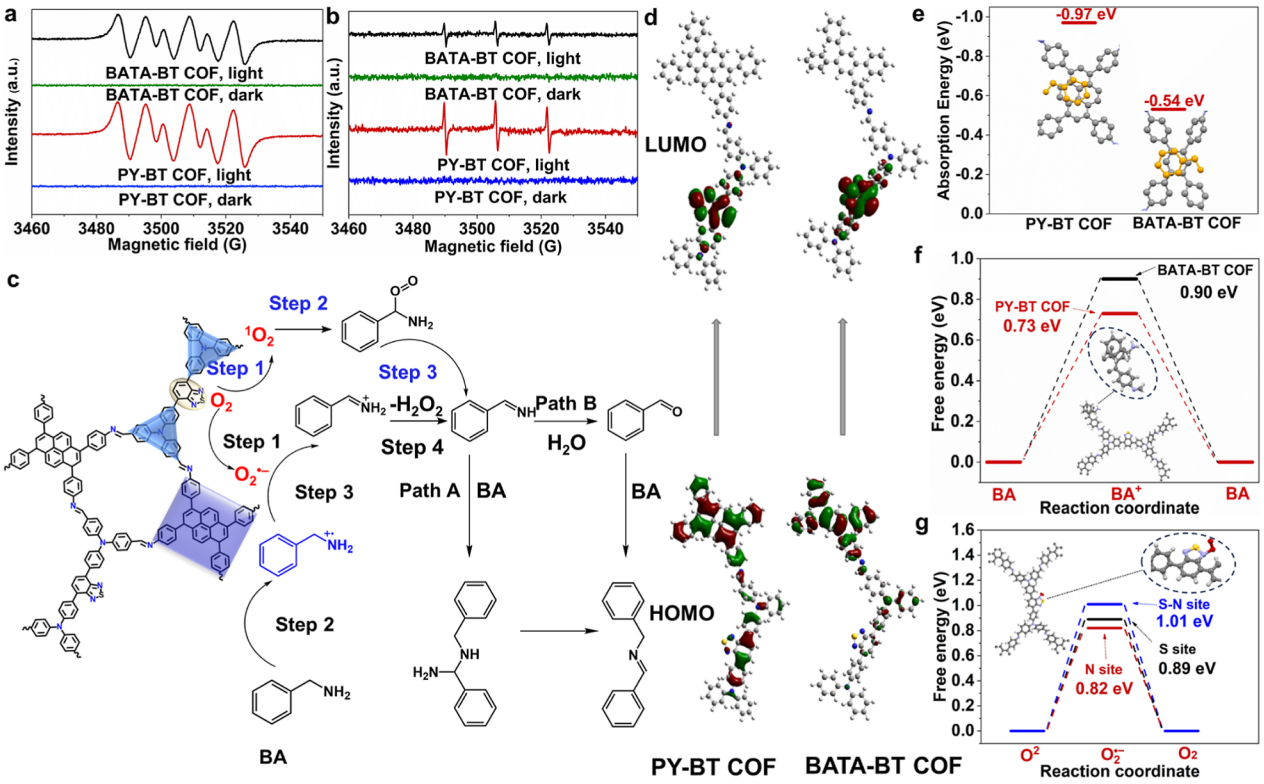

Figure 5. Mechanism and DFT calculations. (a) EPR detection of the generation of $O_2^{\bullet-}$ over the PY-BT COF and BATA-BT COF trapped by DMPO. (b) EPR detection of $^1O_2$ generation over the PY-BT COF and BATA-BT COF trapped by 4-oxo-TEMP. (c) Proposed reaction mechanisms for the photocatalytic benzylamine oxidative coupling reaction. (d) DFT simulation of the HOMO and LUMO of the PY-BT COF and BATA-BT COF. (e) Benzylamine adsorption energy barriers of the PY-BT COF and BATA-BT COF. (f) DFT simulation of the free energy of BA → BA^+ on the PY-BT COF and BATA-BT COF. (g) DFT simulation of the free energy of O_2 → $O_2^{\bullet-}$ on the PY-BT COF.

result generating H_2O_2 and Ph−CH═NH. Similarly, benzylamine is further generated as a final product by the nucleophilic addition reaction of Ph−CH═NH and benzylamine.[62−64]

The DFT calculations further verified the electronic structure and further explored the difference in photocatalytic properties between the PY-BT COF and contrast samples. For the PY-BT COF, the highest occupied molecular orbital (HOMO) site was located mainly at both the pyrene unit and the triphenylamine unit in the ligand, and the lowest unoccupied molecular orbital (LUMO) site lay on the thiadiazole unit. Similarly, the triphenylamine unit in the ligand was attributed to the HOMO and the thiadiazole unit was attributed to the LUMO for the BATA-BT COF, in agreement with the experimental results and the electrochemical band gaps (Figure 5d). The adsorption capacity of benzylamine is also a measurement of the strength of the photocatalytic ability. The results of the adsorption energy for benzylamine by DFT are as follows: the PY-BT COF exhibits −0.97 eV and the BATA-BT COF exhibits −0.54 eV (Figure 5e), indicating that the PY-BT COF has a higher adsorption ability, which is in line with it exhibiting the better photocatalytic activity for benzylamine than the BATA-BT COF. The DFT calculation result also reveals that not only the S atom and the S−N group in the thiadiazole unit but also the N atom in the triphenylamine unit play an important role in adsorbing and activating O_2. The reaction mechanisms for the photocatalytic benzylamine oxidative coupling reaction revealed that the process of O_2 reacts with photogenerated electrons to form $O_2^{\bullet-}$ and energy transfer to form $^1O_2$ would almost appear at the S site and the N site according to the minimum energy principle (Figure 5g). Furthermore, the DFT simulated results showed that the free energy of oxidation coupling reaction of amines for the PY-BT COF was lower than that for other COFs (Figures 5f and S46), further indicating that the PY-BT COF with dual photosensitizer coupled redox molecular junction units was beneficial for promoting the photocatalytic oxidation reaction.

CONCLUSIONS

In summary, this work provided a new strategy for designing multifunctional catalysts by simultaneously introducing different functional units into one structure by covalent linkage. Based on this strategy, we designed a series of three-motif molecular junction type COFs by coupling two photosensitizer units with a redox molecular unit. As a typical catalyst, the PY-BT COF exhibited superior photocatalytic activity with a benzylamine conversion efficiency of 99.9% in 2.5 h, which is much higher that of than other COFs with one photosensitizer with redox molecular junction, a dual photosensitizer with oxidation sites, or one photosensitizer with oxidation site. These results confirmed the superiority of three-motif molecular junction materials. Our results also showed that a covalently linked redox molecular junction can largely enhance the electron transfer efficiency due to the constructed intermolecular charge transfer pathway. This work demonstrated that dual photosensitizer coupled redox molecular junction COFs could work as promising candidates with efficient aerobic oxidation. This is the first report on designing three-motif molecular junction catalysts, which expands the

https://doi.org/10.1021/jacs.3c12724
J. Am. Chem. Soc. 2024, 146, 3396−3404

strategy for structural design of crystalline materials for the catalytic reaction.

■ ASSOCIATED CONTENT

Supporting Information

The Supporting Information is available free of charge at https://pubs.acs.org/doi/10.1021/jacs.3c12724.

Detailed information regarding the experimental methods, characterization analysis, DFT calculations, and simulation for the theoretical COF structure (PDF)

■ AUTHOR INFORMATION

Corresponding Authors

Meng Lu − *School of Chemistry, South China Normal University, Guangzhou 510006, P. R. China;* orcid.org/0000-0003-4502-7517; Email: menglu@m.scnu.edu.cn

Ya-Qian Lan − *School of Chemistry, South China Normal University, Guangzhou 510006, P. R. China;* orcid.org/0000-0002-2140-7980; Email: yqlan@m.scnu.edu.cn; http://www.yqlangroup.com

Authors

Ming-Yi Yang − *School of Chemistry, South China Normal University, Guangzhou 510006, P. R. China*

Shuai-Bing Zhang − *School of Chemistry and Environment Engineering, Changchun University of Science and Technology, Changchun 130022, P. R. China*

Mi Zhang − *School of Chemistry, South China Normal University, Guangzhou 510006, P. R. China*

Ze-Hui Li − *School of Chemistry, South China Normal University, Guangzhou 510006, P. R. China*

Yu-Fei Liu − *School of Chemistry, South China Normal University, Guangzhou 510006, P. R. China*

Xing Liao − *School of Chemistry, South China Normal University, Guangzhou 510006, P. R. China*

Shun-Li Li − *School of Chemistry, South China Normal University, Guangzhou 510006, P. R. China*

Complete contact information is available at: https://pubs.acs.org/10.1021/jacs.3c12724

Author Contributions

All authors have approved the final version of the manuscript. M.-Y. Yang and S.-B. Zhang contributed equally to this paper.

Notes

The authors declare no competing financial interest.

■ ACKNOWLEDGMENTS

This work was supported by the NSFC (no. 22225109, 22071109, 22105080, and 22201083), the National Key R&D Program of China (2023YFA1507204), the Project funded by the China Postdoctoral Science Foundation (no. 2020M682748 and 2021M701270), the Guangdong Basic and Applied Basic Research Foundation (grant 2023A1515010779 and 2023A1515010928), the Guangzhou Basic and Applied Basic Research Fund Project (grant 202102020209), and the China National Postdoctoral Program for Innovative Talents (BX20220115).

■ REFERENCES

(1) Ragauskas, A. J.; Williams, C. K.; Davison, B. H.; Britovsek, G.; Cairney, J.; Eckert, C. A.; Frederick, W. J.; Hallett, J. P.; Leak, D. J.; Liotta, C. L.; Mielenz, J. R.; Murphy, R.; Templer, R.; Tschaplinski, T. The Path Forward for Biofuels and Biomaterials. *Science* **2006**, *311* (5760), 484−489.

(2) Twilton, J.; Le, C.; Zhang, P.; Shaw, M. H.; Evans, R. W.; MacMillan, D. W. C. The merger of transition metal and photocatalysis. *Nat. Rev. Chem* **2017**, *1* (7), 0052.

(3) Yuan, Y. J.; Yu, Z. T.; Chen, D. Q.; Zou, Z. G. Metal-complex chromophores for solar hydrogen generation. *Chem. Soc. Rev.* **2017**, *46* (3), 603−631.

(4) Takata, T.; Jiang, J. Z.; Sakata, Y.; Nakabayashi, M.; Shibata, N.; Nandal, V.; Seki, K.; Hisatomi, T.; Domen, K. Photocatalytic water splitting with a quantum efficiency of almost unity. *Nature* **2020**, *581* (7809), 411−414.

(5) Feng, X. Y.; Pi, Y. H.; Song, Y.; Xu, Z. W.; Li, Z.; Lin, W. B. Integration of Earth-Abundant Photosensitizers and Catalysts in Metal-Organic Frameworks Enhances Photocatalytic Aerobic Oxidation. *ACS Catal.* **2021**, *11* (3), 1024−1032.

(6) Li, Q.; Wang, J.; Zhang, Y.; Ricardez-Sandoval, L.; Bai, G.; Lan, X. Structural and Morphological Engineering of Benzothiadiazole-Based Covalent Organic Frameworks for Visible Light-Driven Oxidative Coupling of Amines. *ACS Appl. Mater. Interfaces* **2021**, *13* (33), 39291−39303.

(7) Han, X. B.; Li, Y. G.; Zhang, Z. M.; Tan, H. Q.; Lu, Y.; Wang, E. B. Polyoxometalate-Based Nickel Clusters as Visible Light-Driven Water Oxidation Catalysts. *J. Am. Chem. Soc.* **2015**, *137* (16), 5486−5493.

(8) Tian, J.; Xu, Z. Y.; Zhang, D. W.; Wang, H.; Xie, S. H.; Xu, D. W.; Ren, Y. H.; Wang, H.; Liu, Y.; Li, Z. T. Supramolecular metal-organic frameworks that display high homogeneous and heterogeneous photocatalytic activity for H_2 production. *Nat. Commun.* **2016**, *7* (1), 11580.

(9) Arnold, P. L.; Ochiai, T.; Lam, F. Y. T.; Kelly, R. P.; Seymour, M. L.; Maron, L. Metallacyclic actinide catalysts for dinitrogen conversion to ammonia and secondary amines. *Nat. Chem.* **2020**, *12* (7), 654−659.

(10) Wang, X.; Chen, L.; Chong, S. Y.; Little, M. A.; Wu, Y.; Zhu, W. H.; Clowes, R.; Yan, Y.; Zwijnenburg, M. A.; Sprick, R. S.; Cooper, A. I. Sulfone-containing covalent organic frameworks for photocatalytic hydrogen evolution from water. *Nat. Chem.* **2018**, *10* (12), 1180−1189.

(11) Tashrifi, Z.; Khanaposhtani, M. M.; Larijani, B.; Mahdavi, M. Recent advances in the oxidative conversion of benzylamines. *Tetrahedron* **2021**, *84*, 131990.

(12) Furukawa, S.; Ohno, Y.; Shishido, T.; Teramura, K.; Tanaka, T. Selective Amine Oxidation Using Nb_2O_5 Photocatalyst and O_2. *ACS Catal.* **2011**, *1* (10), 1150−1153.

(13) Shi, Z.; Li, J.; Han, Q.; Shi, X.; Si, C.; Niu, G.; Ma, P.; Li, M. Polyoxometalate-Supported Aminocatalyst for the Photocatalytic Direct Synthesis of Imines from Alkenes and Amines. *Inorg. Chem.* **2019**, *58* (19), 12529−12533.

(14) Li, S.; Li, G.; Ji, P.; Zhang, J.; Liu, S.; Zhang, J.; Chen, X. A Giant Mo/Ta/W Ternary Mixed-Addenda Polyoxometalate with Efficient Photocatalytic Activity for Primary Amine Coupling. *ACS Appl. Mater. Interfaces* **2019**, *11* (46), 43287−43293.

(15) Li, J.; Chang, B.; Zhao, H.; Meng, Q.; Li, M.; Han, Q. Visible-light-responsive polyoxometalate-based metal-organic framework for highly efficient photocatalytic oxidative coupling of amines. *J. Mater. Sci.* **2021**, *56* (11), 6676−6688.

(16) Marzo, L. P.; Pagire, S. K.; Reiser, O.; König, B. Visible-Light Photocatalysis:Does It Make a Difference in Organic Synthesis? *Angew. Chem., Int. Ed.* **2018**, *57*, 10034−10072.

(17) Liu, Q.; Wu, L. Z. Recent advances in visible-light-driven organic reactions. *Natl. Sci. Rev.* **2017**, *4* (3), 359−380.

(18) Oderinde, M. S.; Frenette, M.; Robbins, D. W.; Aquila, B.; Johannes, J. W. Photoredox Mediated Nickel Catalyzed Cross-Coupling of Thiols With Aryl and Heteroaryl Iodides via Thiyl Radicals. *J. Am. Chem. Soc.* **2016**, *138* (6), 1760−1763.

(19) Liu, N.; Liu, Y.; Liu, Y.; Li, Y.; Cheng, Y.; Li, H. Modulation of photogenerated holes for enhanced photoelectrocatalytic performance. *Microstructures* **2022**, *3* (1), 2023001.

(20) Ding, H.; Li, J.; Xie, G.; Lin, G.; Chen, R.; Peng, Z.; Yang, C.; Wang, B.; Sun, J.; Wang, C. An AIEgen-based 3D covalent organic framework for white light-emitting diodes. *Nat. Commun.* **2018**, *9* (1), 5234.
(21) Cai, S. L.; Zhang, Y. B.; Pun, A. B.; He, B.; Yang, J.; Toma, F. M.; Sharp, I. D.; Yaghi, O. M.; Fan, J.; Zheng, S. R.; Zhang, W. G.; Liu, Y. Tunable electrical conductivity in oriented thin films of tetrathiafulvalene-based covalent organic framework. *Chem. Sci.* **2014**, *5* (12), 4693−4700.
(22) Yu, J.; Liu, Q.; Qiao, W.; Lv, D.; Li, Y.; Liu, C.; Yu, Y.; Li, Y.; Niemantsverdriet, H.; Zhang, B.; Su, R. Catalytic Role of Metal Nanoparticles in Selectivity Control over Photodehydrogenative Coupling of Primary Amines to Imines and Secondary Amines. *ACS Catal.* **2021**, *11* (11), 6656−6661.
(23) Wang, J.; Zhai, Y.; Wang, Y.; Yu, H.; Zhao, W.; Wei, Y. Selective aerobic oxidation of halides and amines with an inorganic-ligand supported zinc catalyst. *Dalton Trans.* **2018**, *47* (38), 13323−13327.
(24) Chen, R.; Shi, J.-L.; Ma, Y.; Lin, G.; Lang, X.; Wang, C. Designed Synthesis of a 2D Porphyrin-Based sp2 Carbon-Conjugated Covalent Organic Framework for Heterogeneous Photocatalysis. *Angew. Chem., Int. Ed.* **2019**, *58* (19), 6430−6434.
(25) Shi, J.-L.; Chen, R.; Hao, H.; Wang, C.; Lang, X. 2D sp2 Carbon-Conjugated Porphyrin Covalent Organic Framework for Cooperative Photocatalysis with TEMPO. *Angew. Chem., Int. Ed.* **2020**, *59* (23), 9088−9093.
(26) Zhi, Y.; Li, Z.; Feng, X.; Xia, H.; Zhang, Y.; Shi, Z.; Mu, Y.; Liu, X. Covalent organic frameworks as metal-free heterogeneous photocatalysts for organic transformations. *J. Mater. Chem. A* **2017**, *5* (44), 22933−22938.
(27) Li, S.; Li, L.; Li, Y. J.; Dai, L.; Liu, C. X.; Liu, Y. Z.; Li, J. N.; Lv, J. N.; Li, P. F.; Wang, B. Fully Conjugated Donor-Acceptor Covalent Organic Frameworks for Photocatalytic Oxidative Amine Coupling and Thioamide Cyclization. *ACS Catal.* **2020**, *10* (15), 8717−8726.
(28) Chang, J. N.; Li, Q.; Shi, J. W.; Zhang, M.; Zhang, L.; Li, S.; Chen, Y. F.; Li, S. L.; Lan, Y. Q. Oxidation-Reduction Molecular Junction Covalent Organic Frameworks for Full Reaction Photosynthesis of H_2O_2. *Angew. Chem., Int. Ed.* **2023**, *62*, No. e202218868.
(29) Zhang, M.; Huang, P.; Liao, J. P.; Yang, M. Y.; Zhang, S. B.; Liu, Y. F.; Lu, M.; Li, S. L.; Cai, Y. P.; Lan, Y. Q. Relative Local Electron Density Tuning in Metal-Covalent Organic Frameworks for Boosting CO_2 Photoreduction. *Angew. Chem., Int. Ed.* **2023**, *62*, No. e202311999.
(30) Chang, J. N.; Shi, J. W.; Li, Q.; Li, S.; Wang, Y. R.; Chen, Y. F.; Yu, F.; Li, S. L.; Lan, Y. Q. Regulation of Redox Molecular Junctions in Covalent Organic Frameworks for H_2O_2 Photosynthesis Coupled with Biomass Valorization. *Angew. Chem., Int. Ed.* **2023**, *62*, No. e2023036.
(31) Zhang, L.; Li, R. H.; Li, X. X.; Liu, J.; Guan, W.; Dong, L. Z.; Li, S. L.; Lan, Y. Q. Molecular oxidation-reduction junctions for artificial photosynthetic overall reaction. *Proc. Natl. Acad. Sci. U. S. A.* **2022**, *119* (40), No. e2210550119.
(32) Li, Q.; Chang, J. N.; Wang, Z. M.; Lu, M.; Guo, C.; Zhang, M.; Yu, T. Y.; Chen, Y. F.; Li, S. L.; Lan, Y. Q. Modulated Connection Modes of Redox Units in Molecular Junction Covalent Organic Frameworks for Artificial Photosynthetic Overall Reaction. *J. Am. Chem. Soc.* **2023**, *145* (42), 23167−23175.
(33) Hu, H.; Yan, Q. Q.; Wang, M.; Yu, L.; Pan, W.; Wang, B. S.; Gao, Y. A. Ionic covalent organic frameworks for highly effective catalysis. *Chin. J. Catal.* **2018**, *39*, 1437−1444.
(34) Su, C. L.; Tandiana, R.; Tian, B. B.; Sengupta, A.; Tang, W.; Su, J.; Loh, K. P. Visible-Light Photocatalysis of Aerobic Oxidation Reactions Using Carbazolic Conjugated Microporous Polymers. *ACS Catal.* **2016**, *6* (6), 3594−3599.
(35) Wu, K.; Liu, X. Y.; Cheng, P. W.; Xie, M.; Lu, W. G.; Li, D. Metal-organic frameworks as photocatalysts for aerobic oxidation reactions. *Sci. China: Chem.* **2023**, *66* (6), 1634−1653.
(36) Yang, X.; Zhang, S. Y.; Li, P. X.; Gao, S. Y.; Cao, R. Visible-light-driven photocatalytic selective organic oxidation reactions. *J. Mater. Chem. A* **2020**, *8* (40), 20897−20924.
(37) Lang, X. J.; Leow, W. R.; Zhao, J. C.; Chen, X. D. Synergistic photocatalytic aerobic oxidation of sulfides and amines on TiO2 under visible-light irradiation. *Chem. Sci.* **2015**, *6* (2), 1075−1082.
(38) Xiong, L. Q.; Tang, J. W. Strategies and Challenges on Selectivity of Photocatalytic Oxidation of Organic Substances. *Adv. Energy Mater.* **2021**, *11* (8), 2003216.
(39) Liu, J.; Gudmundsson, A.; Backvall, J. E. Efficient Aerobic Oxidation of Organic Molecules by Multistep Electron Transfer. *Angew. Chem., Int. Ed.* **2021**, *60* (29), 15686−15704.
(40) Fukuzumi, S.; Lee, Y. M.; Jung, J.; Nam, W. Thermal and photocatalytic oxidation of organic substrates by dioxygen with water as an electron source. *Green Chem.* **2018**, *20* (5), 948−963.
(41) Li, Y.; Chen, W.; Xing, G.; Jiang, D.; Chen, L. New synthetic strategies toward covalent organic frameworks. *Chem. Soc. Rev.* **2020**, *49* (10), 2852−2868.
(42) Huang, N.; Wang, P.; Jiang, D. Covalent organic frameworks: a materials platform for structural and functional designs. *Nat. Rev. Mater.* **2016**, *1* (10), 16068.
(43) Chen, X.; Geng, K.; Liu, R.; Tan, K. T.; Gong, Y.; Li, Z.; Tao, S.; Jiang, Q.; Jiang, D. Covalent Organic Frameworks: Chemical Approaches to Designer Structures and Built-In Functions. *Angew. Chem., Int. Ed.* **2020**, *59* (13), 5050−5091.
(44) Feng, X.; Hu, J. Y.; Redshaw, C.; Yamato, T. Functionalization of Pyrene To Prepare Luminescent Materials-Typical Examples of Synthetic Methodology. *Chem.—Eur. J.* **2016**, *22* (34), 11898−11916.
(45) Gudim, N. S.; Knyazeva, E. A.; Mikhalchenko, L. V.; Golovanov, I. S.; Popov, V. V.; Obruchnikova, N. V.; Rakitin, O. A. Benzothiadiazole vs. iso-Benzothiadiazole: Synthesis, Electrochemical and Optical Properties of D-A-D Conjugated Molecules Based on Them. *Molecules* **2021**, *26* (16), 4931.
(46) Li, J. L.; Zhang, Z. W.; Jia, J.; Liu, X. M. Covalent Organic Frameworks for Photocatalytic Organic Transformation. *Chem. Res. Chin. Univ.* **2022**, *38* (2), 275−289.
(47) Suzuki, K.; Tang, F.; Kikukawa, Y.; Yamaguchi, K.; Mizuno, N. Visible-Light-Induced Photoredox Catalysis with a Tetracerium-Containing Silicotungstate. *Angew. Chem., Int. Ed.* **2014**, *53* (21), 5460−5464.
(48) Shiraishi, Y.; Matsumoto, M.; Ichikawa, S.; Tanaka, S.; Hirai, T. Polythiophene-Doped Resorcinol-Formaldehyde Resin Photocatalysts for Solar-to-Hydrogen Peroxide Energy Conversion. *J. Am. Chem. Soc.* **2021**, *143* (32), 12590−12599.
(49) Heng, S.; Li, L.; Li, W.; Li, H.; Pang, J.; Zhang, M.; Bai, Y.; Dang, D. Enhanced Photocatalytic Hydrogen Production of the Polyoxoniobate Modified with RGO and PPy. *Nanomaterials* **2020**, *10* (12), 2449.
(50) Xu, C.; Liu, H.; Li, D.; Su, J. H.; Jiang, H. L. Direct evidence of charge separation in a metal-organic framework: efficient and selective photocatalytic oxidative coupling of amines via charge and energy transfer. *Chem. Sci.* **2018**, *9* (12), 3152−3158.
(51) Huang, Q.; Liu, J.; Feng, L.; Wang, Q.; Guan, W.; Dong, L. Z.; Zhang, L.; Yan, L. K.; Lan, Y. Q.; Zhou, H. C. Multielectron transportation of polyoxometalate-grafted metalloporphyrin coordination frameworks for selective CO_2-to-CH_4 photoconversion. *Natl. Sci. Rev.* **2020**, *7* (1), 53−63.
(52) He, J.; Han, Q.; Li, J.; Shi, Z.; Shi, X.; Niu, J. Ternary supramolecular system for photocatalytic oxidation with air by consecutive photo-induced electron transfer processes. *J. Catal.* **2019**, *376*, 161−167.
(53) Liu, Y.; Ji, K.; Wang, J.; Li, H.; Zhu, X.; Ma, P.; Niu, J.; Wang, J. Enhanced Carrier Separation in Visible-Light-Responsive Polyoxometalate-Based Metal-Organic Frameworks for Highly Efficient Oxidative Coupling of Amines. *ACS Appl. Mater. Interfaces* **2022**, *14* (24), 27882−27890.
(54) Yusran, Y.; Li, H.; Guan, X.; Fang, Q.; Qiu, S. Covalent Organic Frameworks for Catalysis. *EnergyChem* **2020**, *2* (3), 100035.

https://doi.org/10.1021/jacs.3c12724
J. Am. Chem. Soc. 2024, 146, 3396−3404

(55) Xiao, J.; Liu, X. L.; Pan, L.; Shi, C. X.; Zhang, X. W.; Zou, J. J. Heterogeneous Photocatalytic Organic Transformation Reactions Using Conjugated Polymers-Based Materials. *ACS Catal.* **2020**, *10* (20), 12256−12283.
(56) Li, X. L.; Yang, C. Q.; Sun, B.; Cai, S. L.; Chen, Z. M.; Lv, Y. Q.; Zhang, J.; Liu, Y. Expeditious synthesis of covalent organic frameworks: a review. *J. Mater. Chem. A* **2020**, *8* (32), 16045−16060.
(57) Sun, Q.; Aguila, B.; Ma, S. Q. A bifunctional covalent organic framework as an efficient platform for cascade catalysis. *Mater. Chem. Front.* **2017**, *1* (7), 1310−1316.
(58) Vickers, J. W.; Lv, H.; Sumliner, J. M.; Zhu, G.; Luo, Z.; Musaev, D. G.; Geletii, Y. V.; Hill, C. L. Differentiating Homogeneous and Heterogeneous Water Oxidation Catalysis: Confirmation that $[Co_4(H_2O)_2(\alpha\text{-}PW_9O_{34})_2]^{10-}$ Is a Molecular Water Oxidation Catalyst. *J. Am. Chem. Soc.* **2013**, *135* (38), 14110−14118.
(59) Yu, H.; Wang, J.; Zhai, Y.; Zhang, M.; Ru, S.; Han, S.; Wei, Y. Visible-Light-Driven Photocatalytic Oxidation of Organic Chlorides Using Air and an Inorganic-Ligand Supported Nickel-Catalyst Without Photosensitizers. *ChemCatChem* **2018**, *10* (19), 4274−4279.
(60) Yuan, A.; Lei, H.; Wang, Z.; Dong, X. Improved photocatalytic performance for selective oxidation of amines to imines on graphitic carbon nitride/bismuth tungstate heterojunctions. *J. Colloid Interface Sci.* **2020**, *560*, 40−49.
(61) Huang, Z.; Luo, Z.; Geletii, Y. V.; Vickers, J. W.; Yin, Q.; Wu, D.; Hou, Y.; Ding, Y.; Song, J.; Musaev, D. G.; Hill, C. L.; Lian, T. Efficient Light-Driven Carbon-Free Cobalt-Based Molecular Catalyst for Water Oxidation. *J. Am. Chem. Soc.* **2011**, *133* (7), 2068−2071.
(62) Niu, Q.; Huang, Q.; Yu, T. Y.; Liu, J.; Shi, J. W.; Dong, L. Z.; Li, S. L.; Lan, Y. Q. Achieving High Photo/Thermocatalytic Product Selectivity and Conversion via Thorium Clusters with Switchable Functional Ligands. *J. Am. Chem. Soc.* **2022**, *144* (40), 18586−18594.
(63) Liu, H.; Xu, C. Y.; Li, D. D.; Jiang, H. L. Photocatalytic Hydrogen Production Coupled with Selective Benzylamine Oxidation over MOF Composites. *Angew. Chem., Int. Ed.* **2018**, *57* (19), 5379−5383.
(64) Lv, M.; Tong, F. X.; Wang, Z. Y.; Liu, Y. Y.; Wang, P.; Cheng, H. F.; Dai, Y.; Zheng, Z. K.; Huang, B. B. $BiVO_4$ quadrangular nanoprisms with highly exposed {101} facets for selective photocatalytic oxidation of benzylamine. *J. Mater. Chem. A* **2022**, *10* (37), 19699−19709.

https://doi.org/10.1021/jacs.3c12724
J. Am. Chem. Soc. 2024, 146, 3396−3404